A motion planning algorithm for the rolling-body problem

Le contenu de ce chapitre fait l'objet d'un article en collaboration avec F. Alouges et Y. Chitour, à paraître dans les *IEEE Transactions on Robotics*, volume 26 (2010), numéro 5 (Octobre).

Sommaire

4.1 Introduction

In recent years, nonholonomic systems have attracted much attention due to the theoretical questions raised for their motion planning and to their importance in numerous applications (cf. [69, 75] and references therein). In particular, the planning of robotic manipulators for achieving high operational capability with low constructive complexity is a major issue for the control community in the last decade. Nonholonomy is exploited for the design of such manipulators but ensuring both hardware reduction and controllability performances yields serious difficulties, requiring more elaborate analysis and efficient algorithm. The rolling-body problem illustrates well all the aforementioned aspects.

We recall that the rolling-body problem (without slipping or spinning) is a control system Σ modeling the rolling of a connected surface S_1 on another one S_2 of the Euclidean space $\mathbb{R}^3$ so that the relative speed of the contact point is zero (no slipping) and the relative angular velocity has zero component along the common normal direction at the contact point (no spinning). It is intuitively clear that five parameters are needed to describe the state of Σ : two for parameterizing the contact point as element of S_1, two others for the contact point as

element of S_2, and finally one more parameter for the relative orientation of S_1 with respect to S_2. Therefore, the state space $\mathcal{Q}(S_1, S_2)$ of Σ is a $5-$dimensional manifold and it can be shown that $\mathcal{Q}(S_1, S_2)$ is a circle bundle over $S_1 \times S_2$. Because of the rolling constraints (no slipping, no spinning), one easily shows that, once an absolutely continuous (a.c. for short) curve c_1 on S_1 is prescribed, there exists a unique a.c. curve Γ in $\mathcal{Q}$ describing the rolling without slipping or spinning of the surface S_2 onto the surface S_1 along the curve c_1. Thus, the admissible inputs of the control system Σ exactly correspond to the a.c. curves c_1 of S_1 by their velocities $\dot{c}_1$. As a consequence, Σ can be written (in local coordinates) as a driftless control system of the type $\dot{x} = u_1 F_1(x) + u_2 F_2(x)$, where $(u_1, u_2) \in \mathbb{R}^2$ is the control and F_1, F_2 are vector fields defined in the domain of the chart (cf. [75, 69] and references therein). As regards controllability issues, there exist several works (cf. [69] and references therein) addressing these questions. Agrachev and Sachkov (cf. [2]) proved that Σ is completely controllable if and only if S_1 and S_2 are not isometric. Marigo and Bicchi (cf. [69]) provided geometric descriptions for the possible reachable sets. One of the main conclusions of these works will be instrumental for us and goes as follows : the control system Σ is locally controllable at a point $q \in \mathcal{Q}$ if $K_{S_1}(\mathrm{pr}_1(q)) - K_{S_2}(\mathrm{pr}_2(q)) \neq 0$, where $K_{S_1}(\cdot)$ and $K_{S_2}(\cdot)$ respectively denote the Gaussian curvature of S_1 and S_2, and $\mathrm{pr}_i : \mathcal{Q} \to S_i$, $i = 1, 2$, are the canonical projections. In particular, if S_1 is a strictly convex surface (i.e. $K_{S_1}(q_1) > 0$ for all $q_1 \in S_1$) and $S_2 = \mathbb{R}^2$, then the control system (Σ) is not only completely controllable, but also locally controllable at every point $q \in \mathcal{Q}$. On the opposite direction, it is worth mentioning the following result : Σ is not completely controllable if and only if S_1 and S_2 are isometric, with an isometry of $\mathbb{R}^3$.

Regarding the motion planning problem (MPP for short) associated to the rolling-body problem, most of the attention focused on the rolling of a convex surface S on a flat one, due to the fact that the latter models dexterous robotic manipulation of a convex object by means of a robotic hand with as few as three motors and flat finger, see [69, 75] and references therein. Moreover, in [69], several prototype dexterous grippers are exhibited. Recall that the MPP is the problem of finding a procedure that, for every pair (p, q) of the state space of a control system Σ, *effectively* produces a control $u_{p,q}$ giving rise to an admissible trajectory steering p to q. Note that in the category of rolling-body problem, even the simplest model, the so-called plate-ball system (a sphere rolling on the plane), does not allow any chained-form transformation and is not a flat system. We can hierarchize this category of problems as follows according to increasing level of difficulty :

L1. S_1 rolling on the plane :
- L1-1. the plane is free of prohibited regions ;
- L1-2. there are prohibited regions (obstacles) on the plane ;
- L1-3. there are prohibited regions on S_1 ;

L2. S_1 rolling on the top of S_2 with S_2 non flat, S_1 and S_2 non isometric :
- L2-1. there are prohibited regions neither on S_1 nor on S_2 ;
- L2-2. there are prohibited regions on S_1 or (and) S_2.

For **L1.**, there exists essentially one family of methods commonly called geometric phase methods based on the Gauss-Bonnet Theorem in differential geometry and initiated by Li and Canny. In [66], Li and Canny proposed a first general framework for solving **L1-1**. They devised an ingenious algorithm solving efficiently the MPP of plate-ball problem. However, their method cannot be directly applied to more general convex surfaces S_1 since explicit computation of the integral of the Gaussian curvature over a bounded region on S is in general not available. In the spirit of [66], Bicchi and Marigo proposed in [15] an *approximate* motion planning algorithm solving **L1-1** and **L1-2** for *general* convex body S_1. By using a

lattice structure on the state space, they translated Li-Canny's global and exact computation into a series of local and approximate ones (basic actions), easier to treat in practice. They also showed that this approximate method has good topological properties so that it can be incorporated into a more general motion planning algorithm dealing with obstacles in the plane. However, since a fine-grid lattice is needed in order to improve the precision, a large number of *periodical* maneuvers is necessary for achieving the preassigned change of orientation, producing thus highly oscillating-type motions, which may not be desirable in practice.

In [23], two other approaches to solve **L1-1** were proposed. The first one is based on the Liouvillian character of Σ. One can show that, if S_1 admits a symmetry of revolution, the MPP can be reduced to a purely inverse algebraic problem. However, such an approach presents a serious numerical drawback : the resulting inverse problem requires that implicit functions must be determined through transcendental equations involving local charts for S_1. The second approach proposed in [23] is based on the well-known continuation method (also called homotopy method or continuous Newton's algorithm [4]) which dates back to Poincaré. The MPP is therefore addressed as a pure inverse problem. Let us briefly recall how the continuation method (CM for short) works. It is used for solving nonlinear equations of the form $F(x) = y$, where x is the unknown and $F : X \to Y$ is surjective. Consider $x_0 \in X$ and $y_0 = F(x_0)$. Pick a differentiable path $\pi : [0,1] \to Y$ joining y_0 to the given y. Then, the CM is an iterative procedure which lifts π to a path $\Pi : [0,1] \to X$ so that $F \circ \Pi = \pi$. The word "iterative" refers to the fact that the path Π is obtained by the flow of a differential equation defined on X. Indeed, one starts by differentiating $F(\Pi(s)) = \pi(s)$ to get $DF(\Pi(s))\dot{\Pi}(s) = \dot{\pi}(s)$. The latter is satisfied by setting $\dot{\Pi}(s) := P(\Pi(s))\dot{\pi}(s)$, where $P(x)$ is a right inverse of $DF(x)$. Therefore, solving $F(x) = y$ amounts to first show that $P(\Pi(s))$ exists (for instance if $DF(\Pi(s))$ is surjective) and second to prove that the ODE in X, $\dot{\Pi}(s) = P(\Pi(s))\dot{\pi}(s)$, which is a "highly" non-linear equation (also called the Path Lifting Equation or Wazewski Equation [108]), admits a global solution. In the context of the MPP, the CM was introduced in [35] and [96, 97], and further developed in [25, 24, 29, 102, 103]. The map F is now an end-point map from the space of admissible inputs to the state space. Its singularities are exactly the abnormal extremals of the sub-Riemannian metric induced by the dynamics of the system, which are usually a major obstacle for the CM to apply efficiently to the MPP. In the case of Σ, non trivial abnormal extremals and their trajectories were determined in [23] and they exactly correspond to the horizontal geodesics of Σ. Despite that obstacle, assuming that the surface S is strictly convex and possesses a stable periodic geodesic, it was shown in [23] that the CM provides complete answers to the MPP. More precisely, it was shown that there exist enough paths π in the state space of Σ that can be lifted to paths Π in the control space by showing global existence of solutions to the Wazewski equation.

In this paper, we provide full details for the numerical implementation of the continuation method presented above in order to solve efficiently **L1-1**. The paper is organized as follows : in Section 4.2, we present the kinematic equations of motion of a convex body S_1 *rolling without slipping or spinning* on top of another one S_2. We describe in Section 4.3 how the continuation method can be applied to the motion planning problem. Sufficient conditions guaranteeing the existence of $P(\Pi)$ and the existence of a global solution of the Path Lifting Equation in the case of the rolling-body problem are also reported. Section 4.4 serves to detail some key points for numerical resolution of Path Lifting Equation. In Section 4.5, several numerical simulations are presented. Some detailed comments and possible generalizations will be presented at the end of this paper in Section 4.6.

4.2 Description of the rolling-body problem

In this section, we briefly recall how to derive the equations of motion for the rolling-body problem with no slipping or spinning of a connected surface S_1 of the Euclidean space $\mathbb{R}^3$ on top of another one S_2. This section does not bring new results but we provide it for sake of completeness and also to exhibit the numerical challenges raised by trying to implement ordinary differential equations on a manifold. These results were already obtained in [2, 69, 75].

We start by the intrinsic formulation of the problem, i.e., we first assume that S_1 and S_2 are two-dimensional, connected, oriented, smooth, complete Riemannian manifolds.

4.2.1 Differential geometric notions and definitions

If P is a matrix, we use P^T and $tr(P)$ to denote respectively the transpose of P, and its the trace.

Let $(S, \langle\cdot,\cdot\rangle)$ be a two-dimensional, connected, oriented smooth complete Riemannian manifold for the Riemannian metric $\langle\cdot,\cdot\rangle$. We use TS to denote the tangent bundle over S and US the unit tangent bundle, i.e. the subset of TS of points (x, v) such that $x \in S$ and $v \in T_xS$, $\langle v, v\rangle = 1$.

Let $\{U_\alpha, \alpha\}_{\alpha\in\mathcal{A}}$ be an atlas on S. For $\alpha, \beta \in \mathcal{A}$ such that $U_\alpha \cap U_\beta$ is not empty, we denote by $J_{\beta\alpha}$ the jacobian matrix of $\varphi^\beta \circ (\varphi^\alpha)^{-1}$ the coordinate transformation on $\varphi^\alpha(U_\alpha \cap U_\beta)$. For $\alpha \in \mathcal{A}$, the Riemannian metric is represented by the symmetric definite positive matrix $\mathcal{I}^\alpha$ and set $M^\alpha := \sqrt{\mathcal{I}^\alpha}$.

For $x \in S$, a frame f at x is an ordered basis for T_xS and, for $\alpha, \beta \in \mathcal{A}$, we have $f^\beta = J_{\beta\alpha} f^\alpha$. The frame f is orthonormal if, in addition $M^\alpha f^\alpha$ is an orthogonal matrix. An Orthonormal Moving Frame (briefly OMF) defined on an open subset U of S is a smooth map assigning to each $x \in U$ a positively oriented orthonormal frame $f(x)$ of T_xS.

Let ∇ be the Riemannain connection on S (cf. [91]). For a given OMF f defined on $U \subset S$, the Christoffel symbols associated to $f = (f_1, f_2)$ are defined by

$$\nabla_{f_i} f_j = \sum_k \Gamma_{ij}^k f_k,$$

where $1 \le i, j, k \le 2$. The connection form ω is the mapping defined on U such that, for every $x \in U$, ω_x is the linear application from T_xS to the set of 2×2 skew-symmetric matrices given as follows. For $i, j, k = 1, 2$, the $(i, j)-$th coefficient of $\omega_x(f_k)$ is equal to Γ_{ij}^k.

Let $c : J \to S$ be an absolutely continuous curve in S with J compact interval of $\mathbb{R}$. Set $X(t) := \dot{c}(t)$ in J which defines a vector field along c. Let $Y : J \to TS$ be an absolutely continuous assignment such that, for every $t \in J$, $Y(t) \in T_{c(t)}S$. We say that Y is parallel along c if $\nabla_X Y = 0$ for almost all $t \in J$. In the domain of an OMF f, that equation can be written as follows

$$\dot{Y}^k = -\sum_{1\le i,j\le 2} \Gamma_{ij}^k X^i Y^j,$$

or equivalently,

$$\dot{Y} = -\omega(X)Y.$$

Recall that a curve c is a geodesic if the velocity $\dot{c}(t)$ is parallel along c, that is

$$\nabla_{\dot{c}}\dot{c} = 0. \tag{4.1}$$

4.2.2 Rolling body problem

4.2.2.1 Definition of the state space

Consider now the rolling-body problem with no slipping or spinning of S_1 on top of S_2. We adopt here the viewpoint presented in [2].

At the contact points of the bodies $x_1 \in S_1$ and $x_2 \in S_2$, their tangent spaces are identified by an orientation-preserving isometry

$$q : T_{x_1}S_1 \longrightarrow T_{x_2}S_2,$$

Such an isometry q is a state of the system, and the state space is

$$\begin{aligned} & \mathcal{Q}(S_1, S_2) \\ = \; & \{q : T_{x_1}S_1 \to T_{x_2}S_2 \mid x_1 \in S_1, x_2 \in S_2, q \text{ isometry}\}. \end{aligned}$$

As the set of all orientation-preserving isometries in $\mathbb{R}^2$ is $SO(2)$, which can be identified with the unit circle S^1 in $\mathbb{R}^2$, $\mathcal{Q}(S_1, S_2)$ is a 5-dimensional connected manifold. A point $q \in \mathcal{Q}(S_1, S_2)$ is locally parametrized by $(x_1,\ x_2,\ R)$ with $x_1 \in S_1$, $x_2 \in S_2$ and $R \in SO(2)$.

4.2.2.2 Rolling dynamics

We next describe the motion of one body rolling on top of another one so that the contact point of the first follows a prescribed absolutely continuous (a.c. for short) curve on the second body.

Let f_1 and f_2 be two OMFs defined on the chart domains of α_1, α_2. For $i = 1, 2$, consider a curve $c_i^{\alpha_i}$ defined inside the chart domain α_i on the body S_i. Let $b_i(t) = f_i(c_i(t))R_i(t)$ parallel along $c_i^{\alpha_i}$, $i = 1, 2$, and $R := R_2(t)R_1(t)^{-1} \in SO(2)$ which, by definition, measures the relative position of f_2 with respect to f_1 along $(c_1^{\alpha_1}, c_2^{\alpha_2})$. The variation of R_i along $c_i^{\alpha_i}$, for $i = 1, 2$, is given by $\dot{R}_i = -\omega_i(\dot{c}_i^{\alpha_i})R_i$.

Given an a.c. curve $c_1 : [0, T] \to S_1$, the rolling of S_2 on S_1 without slipping or spinning along c_1 is characterized by a curve $\Gamma = (c_1, c_2, R) : [0, T] \to \mathcal{Q}(S_1, S_2)$ defined the two following conditions.

Up to initial conditions, the no slipping condition amounts to

$$M^{\alpha_2}\dot{c}_2^{\alpha_2}(t) = RM^{\alpha_1}\dot{c}_1^{\alpha_1}(t), \tag{4.2}$$

and the no spinning one to

$$\dot{R}R^{-1} = R\omega_1(\dot{c}_1^{\alpha_1})R^{-1} - \omega_2(\dot{c}_2^{\alpha_2}). \tag{4.3}$$

Since $SO(2)$ is commutative, equation (4.3) reduces to

$$\dot{R}R^{-1} = \omega_1(\dot{c}_1^{\alpha_1}) - \omega_2(\dot{c}_2^{\alpha_2}). \tag{4.4}$$

If we fix a point $x = (x_1, x_2, R_0) \in \mathcal{Q}(S_1, S_2)$, a curve c_1 on S_1 starting at x_1 defines entirely the curve Γ by equations (4.2) and (4.4). Therefore, we can give the following definition :

Definition 4.1. The surface S_2 rolls on the surface S_1 without slipping or spinning if, for every $x = (x_1, x_2, R_0) \in \mathcal{Q}(S_1, S_2)$ and a.c. curve $c_1 : [0, T] \to S_1$ starting at x_1, there exists an a.c. curve $\Gamma : [0, T] \to \mathcal{Q}(S_1, S_2)$ with $\Gamma(t) = (c_1(t), c_2(t), R(t))$, $\Gamma(0) = x$ and for every $t \in [0, T]$, such that, on appropriate charts, equations (4.2) and (4.4) are satisfied. We call the curve $\Gamma(t)$ an admissible trajectory.

If we consider f_1 and f_2 two OMFs and if the state x is represented (in coordinates) by the triple $x = (c_1, c_2, R)$, then for almost all t such that $x(t)$ remains in the domain of an appropriate chart, there exists a measurable function $u(\cdot)$ (called control) with values in $\mathbb{R}^2$ such that

$$\begin{aligned}
\dot{c_1}(t) &= u_1(t) f_1^1(c_1(t)) + u_2(t) f_2^1(c_1(t)), \\
\dot{c_2}(t) &= u_1(t)(f^2(c_2(t))R(t))_1 \\
&\quad + u_2(t)(f^2(c_2(t))R(t))_2, \\
\dot{R}(t)R^{-1}(t) &= \sum_{i=1}^{2} u_i(t)[\omega_1(f_i^1(c_1(t))) \\
&\quad - \omega_2(f^2(c_2(t))R(t))_i].
\end{aligned}$$

Let us consider the vector fields F_1 and F_2 defined by

$$F_i = (f_i^1,\ (f^2 R)_i,\ [\omega_1(f_i^1) - \omega_2(f^2 R)_i])^T, \quad i = 1, 2.$$

Then, the previous system of equations have the following compact form in local coordinates,

$$\dot{x} = u_1 F_1(x) + u_2 F_2(x). \tag{4.5}$$

We recognize the classical form of a driftless control-affine system.

Remark 4.1. In general, it is not possible to get a global basis for the distribution Δ and thus to define globally the dynamics of the control system using vector fields. One notable exception occurs when one of the manifolds is a plane, cf. [23]. Therefore, addressing the motion planning efficiently (i.e. as far as producing a numerical scheme) becomes a delicate issue since most of the standard techniques are based on global vector field expressions of the dynamics of a control system.

The following proposition describes a fundamental property of the rolling problem. For more detail, see [23] for instance.

Proposition 4.1. *Let $u \in H$ be an admissible control that gives rise to the admissible trajectory*

$$\Gamma = (c_1, c_2, R) :\ [0, 1] \to M.$$

Then the following statements are equivalent :

(a) *the curve $c_1 : [0, 1] \to S_1$ is a geodesic ;*
(b) *the curve $c_2 : [0, 1] \to S_2$ is a geodesic ;*
(c) *the curve $\Gamma : [0, 1] \to M$ is a horizontal geodesic.*

Remark 4.2. In the case where S_2 is a plane, if S_1 is rolling along a piecewise linear curve c_2 defined on S_2, then, Proposition 4.1 allows us to construct the locus of the contact point on S_1. Indeed, since S_2 is flat, c_2 is piecewise *geodesic*, it suffices then to integrate a geodesic equation on S_1 to get the locus of the contact point. See Subsection 4.4.3 for more details.

4.2.2.3 Rolling body problem in $\mathbb{R}^3$

From now on, we will assume that the manifolds S_1 and S_2 are oriented surfaces of $\mathbb{R}^3$ with metrics induced by the Euclidean metric of $\mathbb{R}^3$.

We first note that there are two possible ways to define the rolling problem, depending on the respective (global) choice of normal vectors for S_1 and S_2. Indeed, the orientation of the tangents planes of an oriented surface S is determined by the choice of a Gauss map i.e. a continuous normal vector $n : S \to S^2$, with S^2 denoting the sphere of radius 1 in $\mathbb{R}^3$. There are two such normal vectors, n and $-n$. If S is (strictly) convex, these two normal vectors are called inward and outward.

Recall that the rolling-body problem assumes that the tangent spaces at the contact points are identified. In $\mathbb{R}^3$, this is equivalent to identify the normal vectors. Let n_i be the normal vector of S_i, then at contact points, we can either assign n_1 to n_2 or $-n_2$, i.e. we have $n_1 = \varepsilon n_2$ with $\varepsilon = \pm 1$. The physical meaning of this parameter ε is the following : if $\varepsilon = 1$, the two surfaces roll so that one is "inside" the other one, in other words, they are on the same side of their common tangent space at the contact point ; if $\varepsilon = -1$, the two surfaces roll so that one is "outside" the other one, in other words, they are on opposite sides with respect to their common tangent space at the contact point. It is clear that the second situation is more physically feasible in general since, it holds true globally as soon as the two surfaces are convex. We will only deal with this second situation.

We note that Eq. (4.5) has simpler expression in geodesic coordinates. Recall that the geodesic coordinates on a Riemannian manifold S are charts (v, w) defined such that the matrix $\mathcal{I}^\alpha$ is diagonal and equal to $\mathrm{diag}(1, B^2(v, w))$. The function B is defined in an open neighborhood of $(0, 0)$ (the domain of the chart) and satisfies $B(0, w) = 1$, $B_v(0, w) = 0$ and $B_{vv} + K\ B = 0$, where K denotes the Gaussian curvature of S at (v, w) and B_v (B_{vv}, respectively) is the (double, respectively) partial derivative of B with respect to v.

Using the fact that $\mathcal{Q}(S_1, S_2)$ is a circle bundle when S_1 and S_2 are two-dimensional manifolds, and taking geodesic coordinates B_1, B_2 for S_1 and S_2 at contact points x_1 and x_2 respectively, consider coordinates $x = (v_1, w_1, v_2, w_2, \psi)$ in some neighborhood of $(0, \psi_0)$ in $\mathbb{R}^4 \times S^1$. Then, the control system (4.5) can be written locally as

$$\dot{x} = u_1 F_1(x) + u_2 F_2(x), \tag{4.6}$$

with

$$F_1(x) = (1,\ 0,\ \cos\psi,\ -\frac{\sin\psi}{B_2},\ -\frac{B_{2v_2}}{B_2}\sin\psi)^T, \tag{4.7}$$

$$F_2(x) = (0,\ \frac{1}{B_1},\ -\sin\psi,\ -\frac{\cos\psi}{B_2},\ -\frac{B_{1v_1}}{B_1} - \frac{B_{2v_2}}{B_2}\cos\psi)^T, \tag{4.8}$$

see [23] for instance.

Remark 4.3. Since the functions B_1 and B_2 involving in the geodesic coordinates are obtained by solving partial differential equations, the rolling-dynamics given by Eqs. (4.7) and (4.8) is not completely explicit, thus it may not be suitable for numerical implementations. We will explain in Section 4.4 how to overcome this difficulty.

4.3 Continuation method

We start with a general description of the CM, see [25] for more details and complete justifications. The state space $\mathcal{Q}(S_1, S_2)$ is simply denoted by M. The admissible inputs u are elements of $H = L^2([0,1], \mathbb{R}^2)$. We use $\|u(t)\|$ and $\|u\|_H$ respectively to denote $(\sum_{i=1}^2 u_i^2(t))^{1/2}$ and $(\int_0^1 \|u(t)\|^2 dt)^{1/2}$. If $u, v \in H$, then $(u,v)_H = \int_0^1 u^T(t)v(t)dt$.

From the brief description of the continuation method given in the introduction, the map F is equal to the end-point $\phi_p : H \to M$ associated to some fixed $p \in M$. (For more details and complete justifications regarding the continuation method cf. [25].) For $u \in H$ and $p \in M$, let $\gamma_{p,u}$ be the trajectory of Σ starting at p for $t = 0$ and corresponding to u. Then, for $v \in H$, $\phi_p(v)$ is given by

$$\phi_p(v) := \gamma_{p,v}(1).$$

Recall that $\phi_p(v)$ is defined for every $v \in H$. The MPP can be reformulated as follows : for every $p, q \in M$, exhibit a control $u_{p,q} \in H$ such that

$$\phi_p(u_{p,q}) = q. \tag{4.9}$$

In other words, we want to inverse the end-point map ϕ_p, or more precisely, we are looking for a *right-inverse* of ϕ_p as this map is surjective (by the controllability assumption) but not injective ($u_{p,q}$ is not unique). This inversion is performed by using the continuation method summarized in the following scheme.

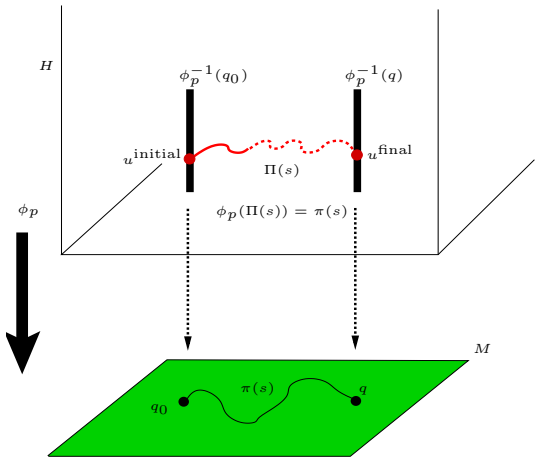

We start with an arbitrary control u^{initial}. Set $q_0 := \phi_p(u^{\text{initial}})$ and choose a path $\pi : [0,1] \to M$ such that $\pi(0) := q_0$ and $\pi(1) := q$. We now look for a path $\Pi : [0,1] \to H$ such that, for every $s \in [0,1]$,

$$\phi_p(\Pi(s)) = \pi(s). \tag{4.10}$$

Differentiating Eq. (4.10) yields to

$$D\phi_p(\Pi(s)) \cdot \frac{d\Pi}{ds}(s) = \frac{d\pi}{ds}(s). \tag{4.11}$$

If $D\phi_p(\Pi(s))$ has full rank, then Eq. (4.11) can be solved for $\Pi(s)$ by taking Π such that

$$\frac{d\Pi}{ds}(s) = P\big(\Pi(s)\big) \cdot \frac{d\pi}{ds}(s), \tag{4.12}$$

where $P(v)$ is a right inverse of $D\phi_p(v)$. For instance, we can choose $P(v)$ to be the Moore-Penrose pseudo-inverse of $D\phi_p(v)$.

We are then led to study the Wazewski equation (4.12) called the Path Lifting Equation (PLE) as an ODE in H. Recall that, by construction, the control defined by $u^{\text{final}} := \Pi(1)$ steers the system from p to q. In order to get the value of $\Pi(1)$, it suffices, at least formally, to solve the following initial value problem defined in the control space H :

$$\begin{cases} \dfrac{d\Pi}{ds}(s) &= P(\Pi(s)) \cdot \dfrac{d\pi}{ds}(s), \\ \Pi(0) &= u^{\text{initial}}. \end{cases} \tag{4.13}$$

Therefore, to successfully apply the CM to the MPP, we have to resolve two issues :

(a) non degeneracy : the path π has to be chosen so that, for every $s \in [0,1]$, $D\phi_p\big(\Pi(s)\big)$ has always full rank ;

(b) non explosion : to solve Eq. (4.9), the PLE defined in Eq. (4.12) must have a global solution on $[0,1]$.

Remark 4.4. Point (a) guarantees the existence of $P(\Pi(s))$ for every $s \in [0,1]$ so that Eq. (4.12) is always well defined. Point (b) is also important since we need to evaluate $\Pi(1)$ to get a control steering the system from p to q.

Remark 4.5. We note that local existence and uniqueness of the solution of the PLE hold as soon as ϕ_p is of class C^2.

It is reasonable to expect difficulties with the singular points of ϕ_p, *i.e.*, the controls $v \in H$ where rank $D\phi_p(v) < 5$ (cf. [18, 72, 27, 28] for general properties of singular points of the end-point map). Let S_p and $\phi_p(S_p)$ be the set of singular points of ϕ_p and the set of singular values respectively. The application of the CM to the MPP is thus decomposed in two steps. In the first one, we have to characterize (when possible) S_p and $\phi_p(S_p)$. The second step consists of lifting paths $\pi : [0,1] \to M$ avoiding $\phi_p(S_p)$ to paths $\Pi : [0,1] \to H$ globally defined on $[0,1]$ by Eq. (4.12).

A sufficient condition resolving (a) and (b) is given by

Condition 4.1. *We say that a closed subset $\mathcal{K}$ of M verifies Condition 4.1 if*

(i) $\mathcal{K}$ is disjoint from $\overline{\phi_p(S_p)}$, where $\overline{\phi_p(S_p)}$ is the closure of $\phi_p(S_p)$;

(ii) there exists $c_{\mathcal{K}} > 0$ such that, for every $u \in H$ with $\phi_p(u) \in \mathcal{K}$, we have

$$\|P(u)\| \leq c_{\mathcal{K}} \|u\|, \tag{4.14}$$

where

$$\|P(u)\| = \Big(\inf_{\|z\|=1} z^T D\phi_p(u) D\phi_p(u)^T z\Big)^{-1/2},$$

with $z \in T^*_{\phi_p(u)}M$.

Once the existence of a closed set $\mathcal{K}$ verifying the **Condition 4.1** is guaranteed, an application of Gronwall Lemma yields that, for every path $\pi : [0,1] \to \mathcal{K}$ of class C^1 and every control $\bar{u} \in H$ such that $\phi_p(\bar{u}) = \pi(0)$, the solution of the PLE defined in Eq. (4.12) with initial condition $\bar{u}$ exists globally on the interval $[0,1]$.

We now consider the MPP of a strictly convex surface S_1 rolling on the on a plane. It is shown in [23] that if S_1 verifies a simple geometric property (see **Condition 4.2** in Appendix), then there exists a compact subset $\mathcal{K}$ in M verifying the **Condition 4.1**, which is large enough to completely resolve the MPP. The reader can refer to Appendix for a

summary of the results regarding the set $\mathcal{K}$ for the rolling-body problem, and a complete development on this issue can be found in [23].

For numerical purposes, we recall here the structure of S_p and $\phi_p(S_p)$ for the rolling-body problem. A proof can be found in [23] for instance.

Proposition 4.2. *For $p \in M$, one has*

$$S_p = \{(v\cos\theta, v\sin\theta) | v \in L^2([0,1],\mathbb{R}), \theta \in [0,2\pi]\},$$

and $\phi_p(S_p)$ is equal to the union of the end-points of all horizontal geodesics starting at p, i.e. all trajectories starting at p and corresponding to one control $u \in S_p$.

In other words, Proposition 4.2 states that singular controls in the case of convex surfaces rolling on the plane are exactly straight lines on the plane.

4.4 Numerical implementation

In this section, we describe how the continuation method can be implemented in order to solve numerically the MPP for rolling-bodies in the case where S_1 is a strictly convex surface of $\mathbb{R}^3$ and S_2 is the Euclidean plane $\mathbb{R}^2$. In that case, the dynamics of the control system is given in geodesic coordinates by

$$\begin{aligned}
\dot{v}_2 &= u_1, \\
\dot{w}_2 &= u_2, \\
\dot{v}_1 &= \cos\psi u_1 - \sin\psi u_2, \\
\dot{w}_1 &= -\frac{1}{B}\sin(\psi)u_1 - \frac{1}{B}\cos(\psi)u_2, \\
\dot{\psi} &= -\frac{B_{v_1}}{B}\sin(\psi)u_1 - \frac{B_{v_1}}{B}\cos(\psi)u_2,
\end{aligned} \tag{4.15}$$

where we use B to denote the function occurring in the definition of geodesic coordinates on S_1. Note that Eq. (4.15) is deduced from Eq. (4.6) by assuming that S_2 is flat.

For the sake of simplicity, we make assumption that S_1 is defined as one bounded connected component of the zero-level set of a smooth real-valued function $f : \mathbb{R}^3 \to \mathbb{R}$. The normal vector field to S_1 is denoted by $n : S_1 \to S^2$ and is given in that case by

$$\frac{\nabla f}{\|\nabla f\|},$$

where $\nabla f = (f_x, f_y, f_z)$ denotes the gradient vector of f. The Gaussian curvature of S_1 is denoted by K and we assume that $K_{min} := \min_{S_1} K > 0$. In addition, set $K_{max} := \max_{S_1} K$.

In the sequel, we still use H and M to denote respectively the control space and the state space of the control system defined by Eq. (4.15). From Section 4.3, we deduce the following motion planning algorithm which, for any pair $(p, q) \in M \times M$, produces an input u^{final} steering the control system (4.15) from p to q.

Note that the only difficulty in **Algorithm 1** is step (iii), requiring to solve numerically an ordinary differential equation defined on the control space H which is in general an infinite dimensional vector space. In the following paragraphs, we detail some key points for solving Eq. (4.16).

Algorithm 9 Motion Planning Algorithm

(i) Choose an arbitrary non singular control $u^{\text{initial}} \in H$ such that $\text{pr}_1(q_0) = \text{pr}_1(q)$ where $q_0 := \phi_p(u^{\text{initial}})$.

(ii) Define a curve $\pi : [0,1] \to M$ such that $\pi(0) := q_0$ and $\pi(1) := q$.

(iii) Solve numerically the following initial value problem

$$\begin{cases} \dfrac{d\Pi}{ds}(s) &= P(\Pi(s)) \cdot \dfrac{d\pi}{ds}(s), \\ \Pi(0) &= u^{\text{initial}}. \end{cases} \tag{4.16}$$

(iv) Set $u^{\text{final}} := \Pi(1)$.

4.4.1 Discretizing the control space H

We start by approximating the control space H which is an infinite dimensional vector space. Recall that in our case controls are just plane curves $c_2 : [0,1] \to \mathbb{R}^2$ such that $\dot{c}_2 = (u_1, u_2)$ for almost all $t \in [0,1]$. We divide the interval $[0,1]$ into N parts, and we approximate the control space H by the $2N$-dimensional subspace $\hat{H}$ of piecewise linear functions. Then, c_2 can be approximated by $\hat{c}_2$, the linear interpolation of $(c_2^1, \ldots, c_2^N)$ where $c_2^i = c_2(\frac{i}{N-1}) = (x_i, y_i)^T$. On each segment $[t_i, t_{i+1}] = [\frac{i}{N-1}, \frac{i+1}{N-1}]$, the approximate control $(\hat{u}_1^i, \hat{u}_2^i)^T$ is proportional to the vector $(x_{i+1} - x_i, y_{i+1} - y_i)^T$.

Remark 4.6. We have chosen the space of piecewise linear functions as the approximate control space for two reasons : (i) piecewise linear curves are easy to be implemented on the plane ; (ii) the corresponding trajectories on S_1 are also easy to be obtained by integrating some geodesic equations by using Proposition 4.1 (see also Remark 4.2), instead of Eq. (4.15) where the function B defining the geodesic coordinates is not given explicitly. This second point plays a crucial role in improving the efficiency of our method. More details will be given in Subsection 4.4.3.

Remark 4.7. We note that elements in $\hat{H}$ are *piecewise* linear functions with more than one piece, then they are not singular inputs. See also Proposition 4.2.

The Path Lifting Equation (4.12) tells us how we have to modify this piecewise constant control $(\hat{u}_1, \hat{u}_2)$ in order to obtain an appropriate control steering our system from an initial state to a preassigned final state. Under some general geometric assumptions for S_1, theoretical results presented in Section 4.3 guarantee that, whatever the starting control we choose, Eq. (4.12) is complete and provides the correct control law at the end of the integration. We use the classical Euler scheme to integrate Eq. (4.12). Note that Theorem 1 in [25] ensures that, once there exists a global solution to Eq. (4.12), then for any "reasonable" Galerkin approximation of the control space and "reasonable" numerical scheme for the derivatives, there exists a global solution for the corresponding numerical approximation of Eq. (4.12).

In the following two paragraphs, we give details about the two key points for the numerical implementation which are the evaluation of a right inverse of $D\phi_p(u)$ and the integration of Eq. (4.15).

4.4.2 Computing $D\phi_p(u)$

We first need to define a field of covectors along $\gamma_{p,u}$. For $z \in T^*_{\phi_p(u)}M$, let $\lambda_{z,u} : [0,1] \to T^*M$ be the field of covectors along $\gamma_{p,u}$ satisfying (in coordinates) the adjoint equation along

$\gamma_{p,u}$ with terminal condition z, *i.e.*, $\lambda_{z,u}$ is a.c., $\lambda_{z,u}(1) = z$ and for a.e. $t \in [0,1]$,

$$\dot{\lambda}_{z,u}(t) = -\lambda_{z,u}(t) \cdot \left(\sum_{i=1}^{2} u_i(t) DF_i(\lambda_{z,u}(t)) \right). \tag{4.17}$$

If X is a smoothvector field over M, the switching function $\varphi_{X,z,u}(t)$ associated to X is the evaluation of $\lambda \cdot X(x)$, the Hamiltonian function of X along $(\gamma_{p,u}, \lambda_{z,u})$, *i.e.*, for $t \in [0,1]$,

$$\varphi_{X,z,u}(t) := \lambda_{z,u}(t) \cdot X(\gamma_{p,u}(t)),$$

(see for instance [25] for more details). Then $D\phi_p(u)$ can be computed as follows : for $z \in T^*_{\phi_p(u)}M$ and $u, v \in H$,

$$z \cdot D\phi_p(u)(v) = (v, \varphi_{z,u})_H, \tag{4.18}$$

where the switching function vector $\varphi_{z,u}(t)$ is the solution of the following Cauchy problem, defined (in coordinates) below, by (cf. [23])

$$\begin{array}{rcl} \dot{\varphi}_1 &=& -u_2 K \varphi_3, \\ \dot{\varphi}_2 &=& u_1 K \varphi_3, \\ \dot{\varphi}_3 &=& -u_2 \varphi_4 + u_1 \varphi_5, \\ \dot{\varphi}_4 &=& -u_2 K \varphi_3, \\ \dot{\varphi}_5 &=& u_1 K \varphi_3. \end{array} \tag{4.19}$$

with terminal condition $\varphi_{z,u}(1) = z$. The reader is referred to [73, Sections 5.2.2 and 5.2.3] for a detailed computation of the differential of the end-point map in general.

In practice, since the discrete $D\phi_p(u)$ is a 5×5 matrix and its image is given by Eq. (4.18), it suffices to take five independents vectors in $\mathbb{R}^5$ as final conditions z, for instance the five elements in the canonical basis of $\mathbb{R}^5$ and integrate Eq. (4.19) in reverse time.

In our simulations, a fourth-order Runge-Kutta numerical scheme is used for integration, the scalar product $(\cdot,\cdot)_H$ in control space H is evaluated by Gaussian quadrature and the Gaussian curvature K is computed by using the following proposition, cf. [13].

Proposition 4.3. *Let S be (a bounded connected component of) the zero-set of $f : \mathbb{R}^3 \to \mathbb{R}$, and define a, b, c by*

$$\det \begin{pmatrix} \nabla^2 f - \lambda I_3 & \nabla f \\ (\nabla f)^T & 0 \end{pmatrix} = a + b\lambda + c\lambda^2, \tag{4.20}$$

where $\nabla^2 f$ is the matrix of the second derivatives of f and I_3 the identity 3×3 matrix.

With this notation, one has

$$K = \frac{a/c}{\|\nabla f\|^2}. \tag{4.21}$$

Explicit computations show that $c = -\|\nabla f\|^2$ and

$$a = \det \begin{pmatrix} \nabla^2 f & \nabla f \\ (\nabla f)^T & 0 \end{pmatrix}.$$

Hence, we have

$$K = -\frac{\det \begin{pmatrix} \nabla^2 f & \nabla f \\ (\nabla f)^T & 0 \end{pmatrix}}{\|\nabla f\|^4}. \tag{4.22}$$

The gradient vector ∇f is then evaluated by a classical right-shifting finite difference scheme, and $\nabla^2 f$ by a centered one. For example, if $X = (x, y, z)$, then $f_x(X)$ is given by

$$\frac{f(x+\varepsilon, y, z) - f(x, y, z)}{\varepsilon}, \tag{4.23}$$

and $f_{xx}(X)$ by

$$\frac{f(x+\varepsilon, y, z) - 2f(x, y, z) + f(x-\varepsilon, y, z)}{\varepsilon^2}, \tag{4.24}$$

with $\varepsilon > 0$ small enough.

4.4.3 Lifting the plane curve $\hat{c}_2$ on S_1

Note that the curvature K appearing in Eq. (4.19) is taken at the final contact point on the surface S_1 after it has rolled along the piecewise constant curve $\hat{c}_2$. Thus, in order to locate the final point, we need to "lift" the plane curve $\hat{c}_2$ on S_1, and the lifting dynamics are given by Eq. (4.15). However, since the geodesic coordinates involved in Eq. (4.15) are not given explicitly in practice, our numerical *lifting* method is based on Proposition 4.1. See also Remark 4.2.

On each interval $[t_i, t_{i+1}]$, the approximate control curve $\hat{c}_2$ is a straight line (i.e. a geodesic in $\mathbb{R}^2$), and then, by Proposition 4.1, the lifting curve $\hat{c}_1$ on S_1 is also a geodesic on each interval $[t_i, t_{i+1}]$ for all $i = 0, \dots, N-1$. Then, from the initial contact point X_0 on S_1, we can integrate successively the geodesic equation on each $[t_i, t_{i+1}]$ with initial conditions equal to $\hat{c}_1(t_i)$ and $(\hat{u}_1^i, \hat{u}_2^i)$, for $i = 0, \dots, N-1$.

Let us write explicitly the geodesic equation to be integrated (see for instance [13] for more details). Recall that a curve $c : [0, 1] \to S_1$ is a geodesic curve if it verifies Eq. (4.1). In the case where S_1 is an immersed surface in $\mathbb{R}^3$, Eq. (4.1) is equivalent to

$$\ddot{c}(t) \perp T_{c(t)} S_1, \tag{4.25}$$

for almost all t in $[0, 1]$.

When S_1 is defined as (a bounded connected component of) the zero-level set of a real-valued function $f : \mathbb{R}^3 \to \mathbb{R}$, we have $\nabla f(x) \perp T_x S_1$ at every $x \in S_1$. Thus, Eq. (4.25) becomes

$$\ddot{c} = \left\langle \ddot{c}, \frac{\nabla f(c)}{\|\nabla f(c)\|} \right\rangle \frac{\nabla f(c)}{\|\nabla f(c)\|}, \tag{4.26}$$

where $\langle , \rangle$ is the scalar product in $\mathbb{R}^3$.

Furthermore, since c is a curve traced on S_1, we also have

$$\langle \dot{c}(t), \nabla f(c(t)) \rangle = 0, \tag{4.27}$$

for almost all t in $[0, 1]$. Then, by deriving Eq. (4.27) with respect to t, we get

$$\langle \ddot{c}, \nabla f(c) \rangle + \langle \dot{c}, \nabla^2 f(c) \dot{c} \rangle = 0. \tag{4.28}$$

Finally, summing up Eq. (4.26) and Eq. (4.28) together, we get

$$\ddot{c} = -\frac{\dot{c}^T \nabla^2 f(c) \dot{c}}{\|\nabla f(c)\|^2} \nabla f(c). \tag{4.29}$$

We use again a fourth-order Runge-Kutta scheme for numerical integration of Eq. (4.29).

An additional difficulty is that the numerical integration is not performed in an Euclidean space, but on a manifold S_1. Assume that we are at point $x \in S_1$ at time t. Then, at time $t + \delta t$, we move to $X_{\text{new}} = X + (\delta t)d$ with $d \in T_x S_1$, but X_{new} does not belong to S_1 if d is nonzero. Therefore, at each integration step, we have to "project" X_{new} on S_1.

More precisely, assume that the point $(0, 0, 0)$ is inside the convex body S_1. Since S_1 is defined as (a bounded connected component of) the zero-level set of a smooth function f, we assume that $|f(X_{\text{new}})| \leq \varepsilon$ for some $\varepsilon << 1$, i.e X_{new} is close to S_1. Then, there exists a unique real number μ close to 1 such that $f(\mu X_{\text{new}}) = 0$, as a simple consequence of the convexity of S_1. The "projection" issue to be addressed is clearly a local one and therefore, Newton's method is efficient for finding μ. The derivative with respect to μ is also needed, it is evaluated by a finite difference scheme similar to Eq. (4.23).

4.5 Simulations

We have applied the numerical continuation method presented above for motion planning problem of several bodies rolling on the Euclidean plane. We first present the rolling of a flattened ball and an egg. We then give simulation in a case where the rolling body does not have a symmetry of revolution. Still, the CM works quite efficiently.

Let us point out that we have written a Matlab program which provided us with the figures presented below. In particular, these figures contain buttons and windows of the Matlab interface. For the convenience of the reader, we will recall all the equations defining the rolling surfaces in the corresponding paragraphs. All the figures show the starting and ending contact points and orientations in the top left, the current trajectory on the plane together with the starting and ending configurations of the rolling body in the top right, and the corresponding trajectory on the body in the bottom left. Since the key point is to show how the continuation method modifies smoothly an arbitrary non singular plane curve to achieve a "right" one, for each test case, we show in the first figure the initial curve that we have chosen, in the second and third figures two intermediate phases adjusting the contact point and orientation, in the fourth figure, the final curve computed by the algorithm as well as the body rolling along this curve, and finally, in the last figure, the matching between the real final state and the preassigned one.

We also note that the computation time is on average 30 seconds (2.2 GHz Intel Core 2 Duo, 1.6 G memory) for 70 iterations with $N = 100$ for the discretization of control space H.

4.5.1 Flattened ball rolling on the plane

This flattened ball is defined by the zero-level set of the function

$$f(x, y, z) = x^2 + y^2 + 5z^2 - 1. \tag{4.30}$$

The gradient $\nabla f(x, y, z)$ is equal to $(2x, 2y, 10z)^T$. One can check that it is never equal to zero on the zero-level set of Eq. (4.30). Then Eq. (4.22) and Eq. (4.29) are always well defined.

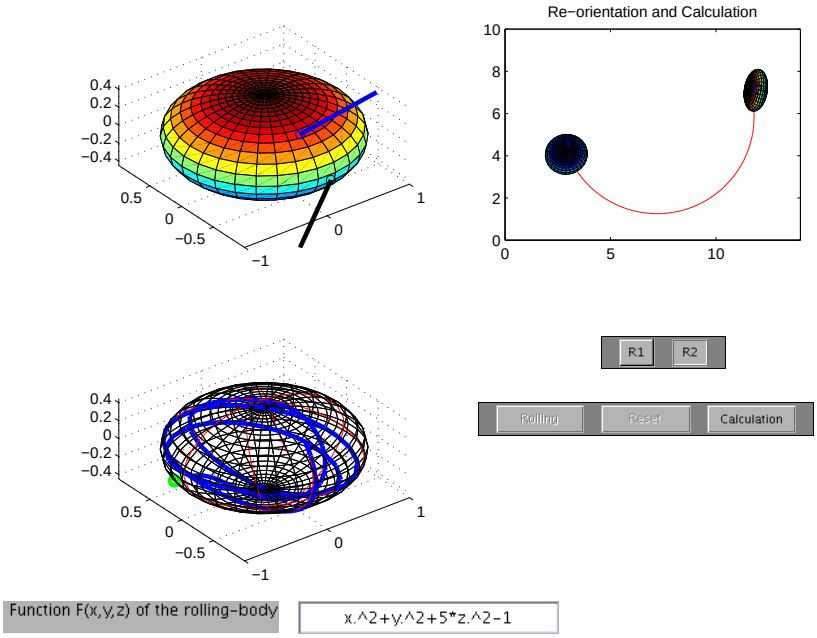

FIGURE 4.1 – Initial and final positions of contact point and orientations of the flattened ball ($s = 0$).

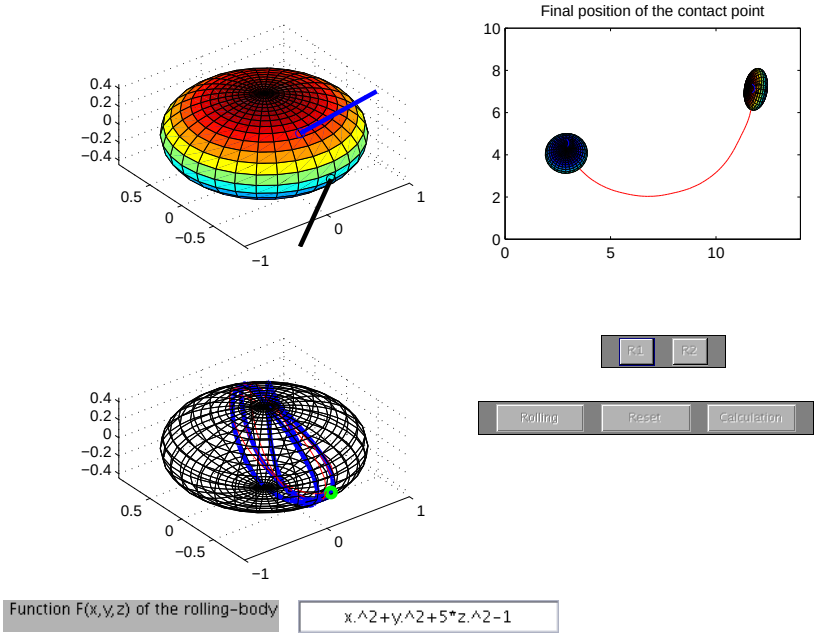

FIGURE 4.2 – Computation for adjusting the final position of contact point by continuation method ($s = 35$).

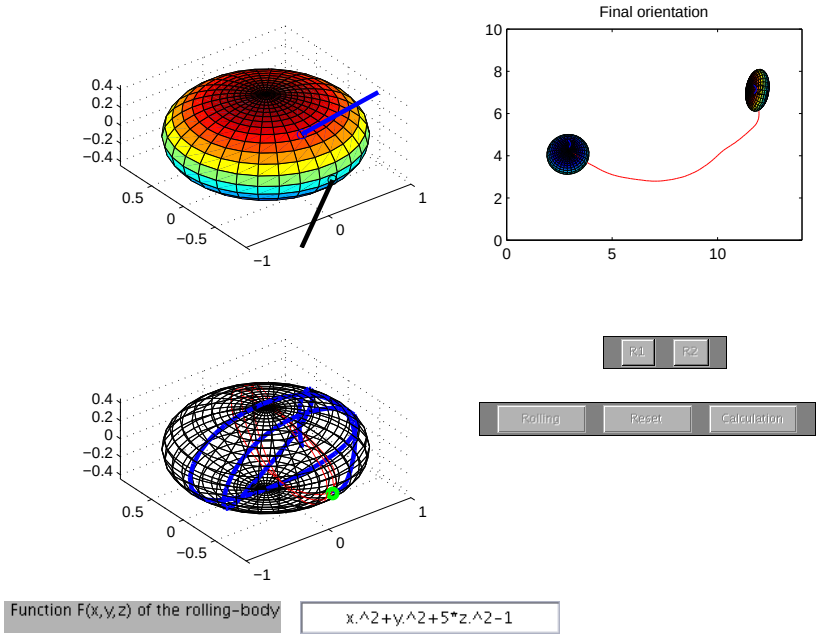

FIGURE 4.3 – Computation for adjusting the final orientation of the flattened ball by continuation method ($s = 70$).

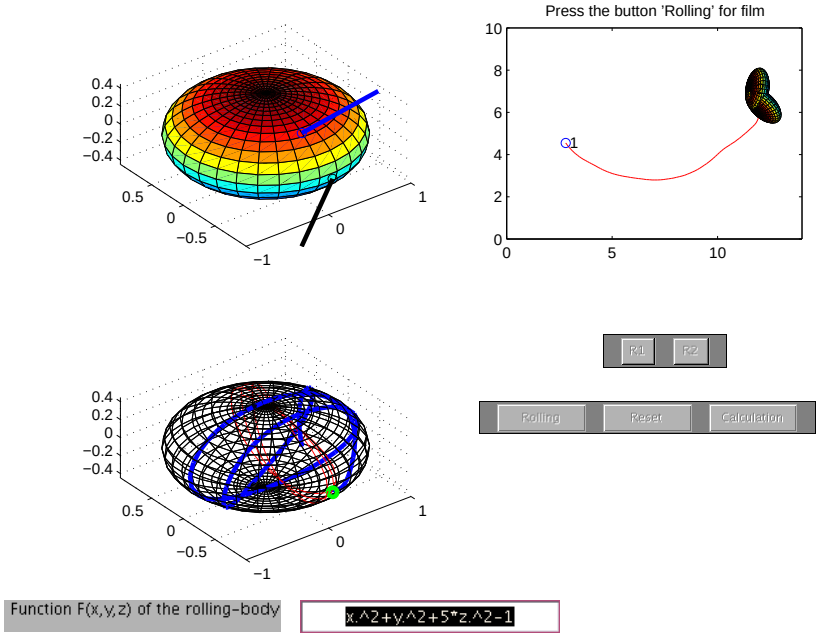

FIGURE 4.4 – Flattened ball rolling along the curve before reaching the final position.

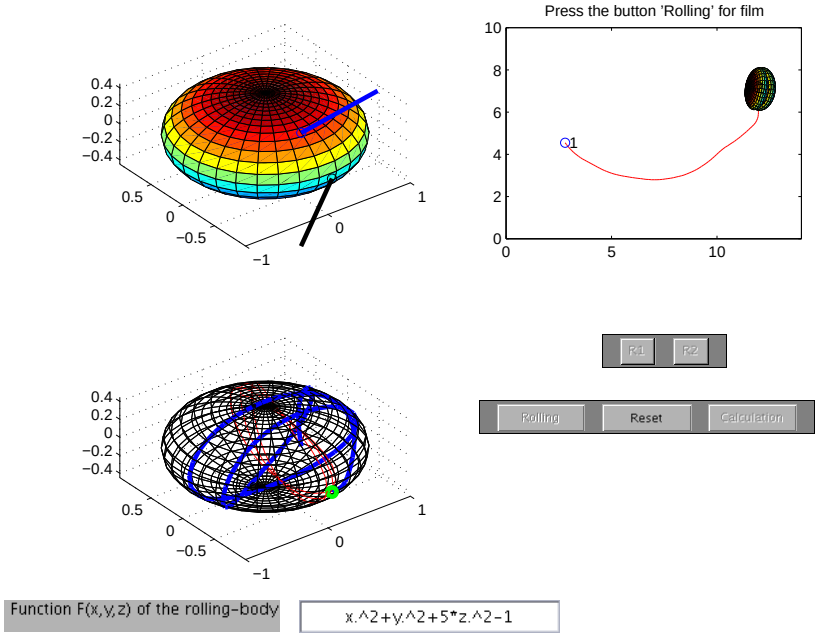

FIGURE 4.5 – Matching at the end of rolling.

4.5.2 Egg rolling on the plane

This "egg" is defined by one bounded connected component of the zero-level set of the function

$$f(x,y,z) = \frac{x^2+y^2}{1-0.4z} + \frac{z^2}{4} - 1. \tag{4.31}$$

We note that $\nabla f(x,y,z) = (\frac{2x}{1-0.4z}, \frac{2y}{1-0.4z}, \frac{0.4(x^2+y^2)}{(1-0.4z)^2} + \frac{z}{2})^T$. One can check that it is never equal to zero on the zero-level set of Eq. (4.31) and therefore Eq. (4.22) and Eq. (4.29) are always well defined.

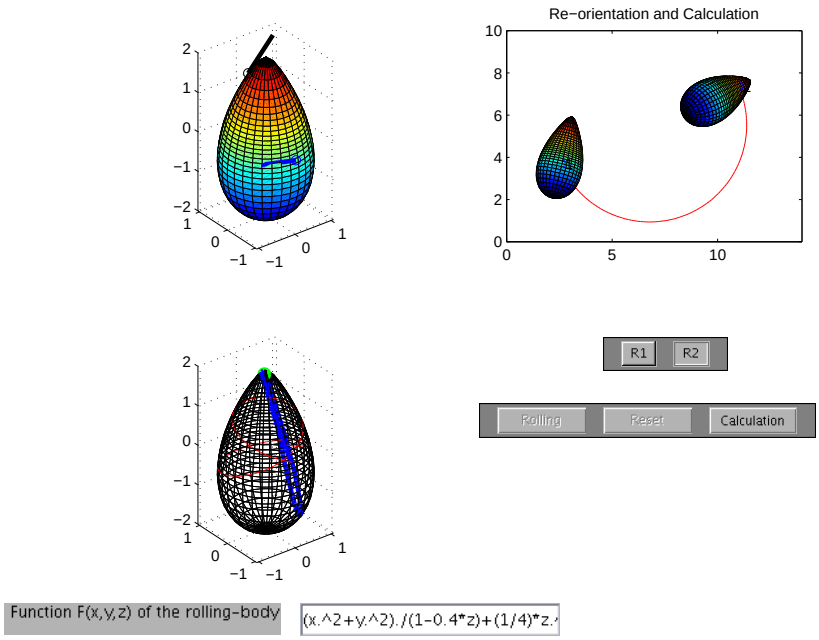

FIGURE 4.6 – Initial and final positions of contact point and orientations of the egg ($s = 0$).

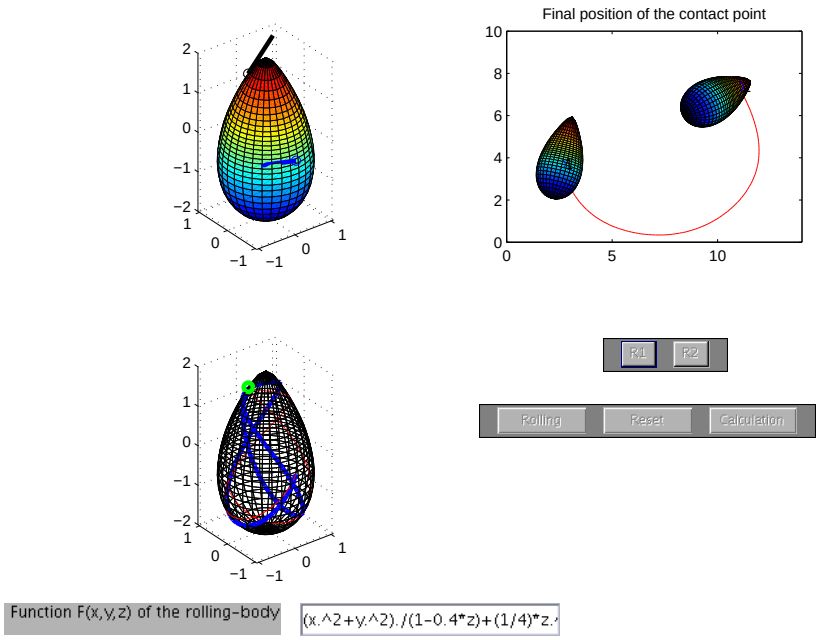

FIGURE 4.7 – Computation for adjusting the final position of contact point by continuation method ($s = 35$).

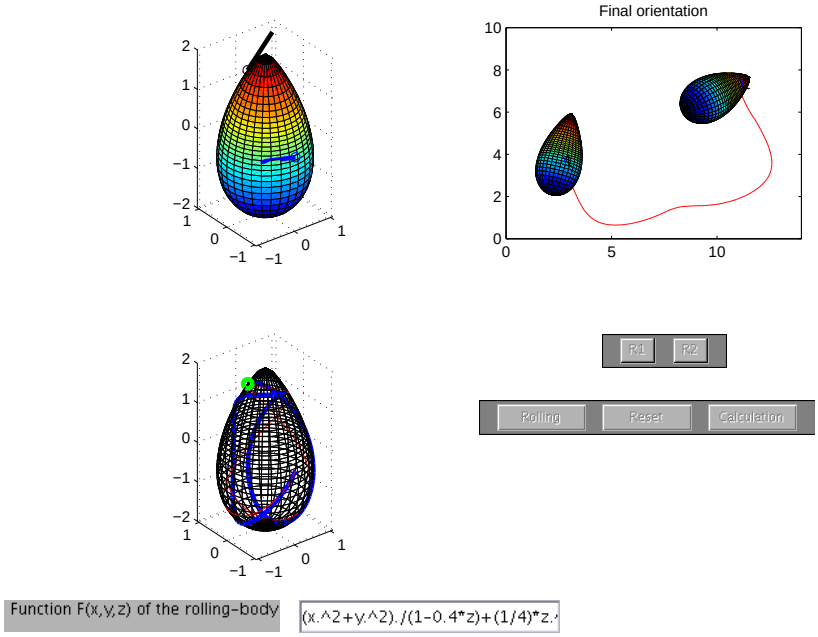

FIGURE 4.8 – Computation for adjusting the final orientation of the egg by continuation method ($s = 70$).

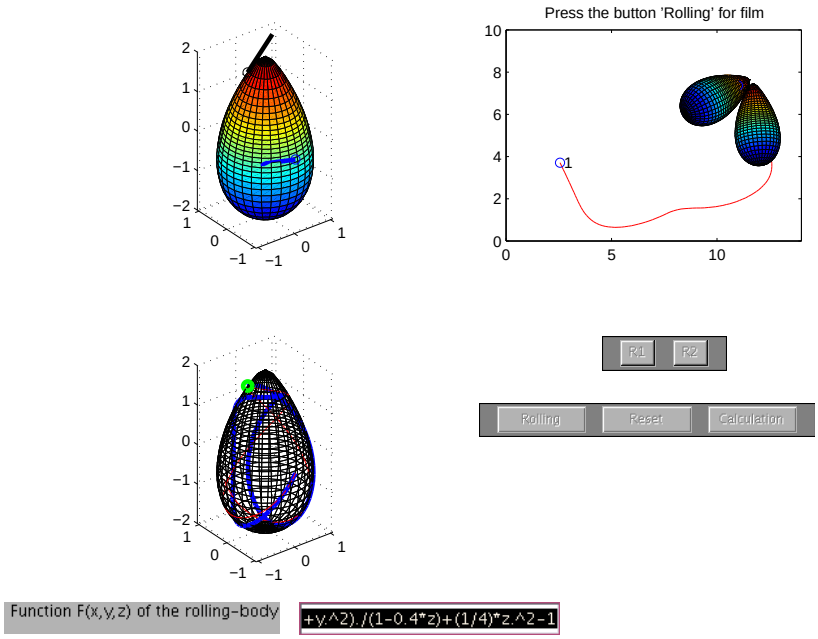

FIGURE 4.9 – Egg rolling along the curve before reaching the final position.

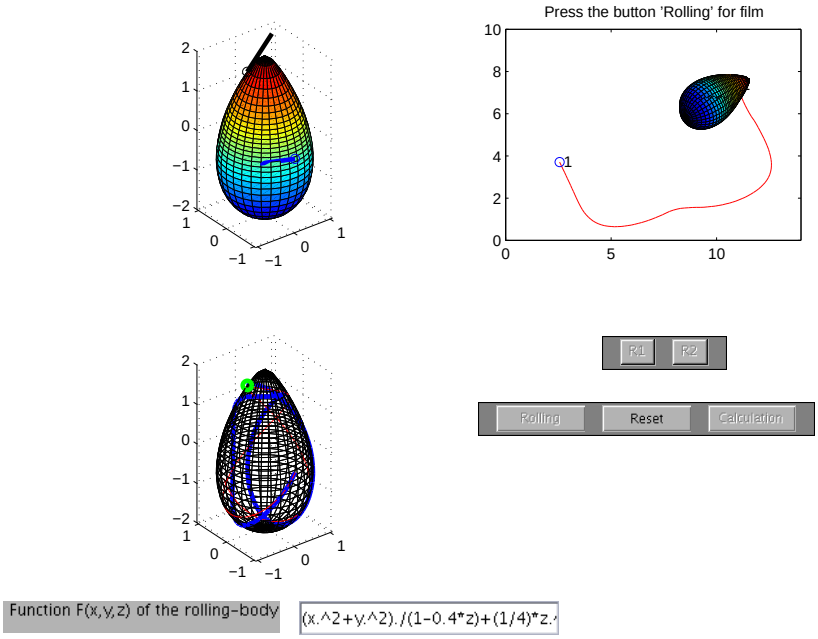

FIGURE 4.10 – Matching at the end of rolling.

4.5.3 More general case

In Section 4.3, the global convergence of continuation method has been proven for rolling of convex body with symmetric axis. However, we show in the subsequent simulations that the continuation method still works numerically in more general cases, even though a theoretical convergence result is not available. This illustrates the robustness of the method.

For example, we take the convex body without symmetric axis, defined by one bounded connected component of the zero-level set of the function

$$f(x,y,z) = \frac{x^2}{1-0.5y} + \frac{2y^2}{1-0.1z} + \frac{0.5z^2}{1-0.3x-0.1y} - 1. \tag{4.32}$$

We note that

$$\nabla f(x,y,z) = \begin{pmatrix} \frac{2x}{1-0.5y} + \frac{0.3}{(1-0.3x-0.1y)^2} \\ \frac{4y}{1-0.1z} + \frac{0.1}{(1-0.3x-0.1y)^2} \\ \frac{0.2y^2}{(1-0.1z)^2} + \frac{z}{1-0.3x-0.1y} \end{pmatrix}.$$

One can check that it is never equal to zero on the zero-level set of Eq. (4.32) and therefore Eq. (4.22) and Eq. (4.29) are always well defined.

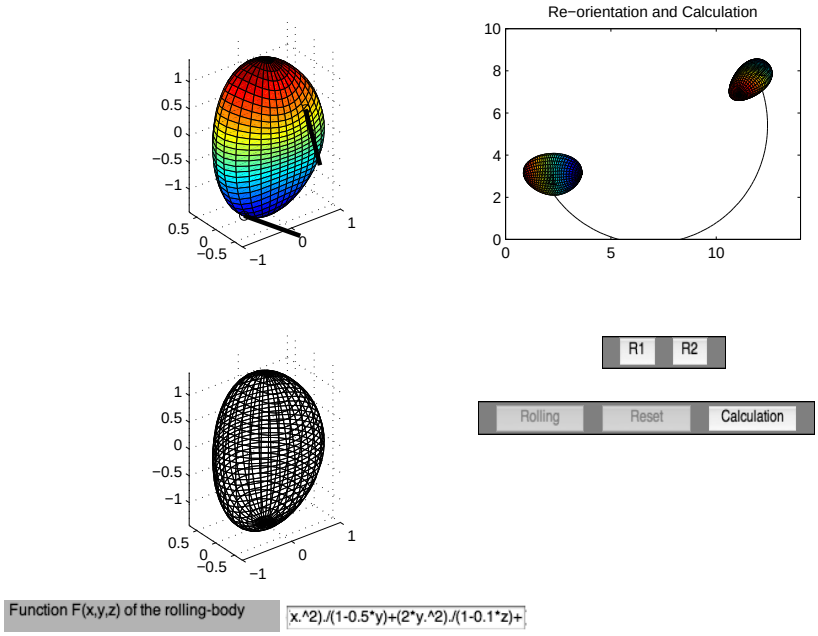

FIGURE 4.11 – Initial and final positions of contact point and orientations of the convex body ($s = 0$).

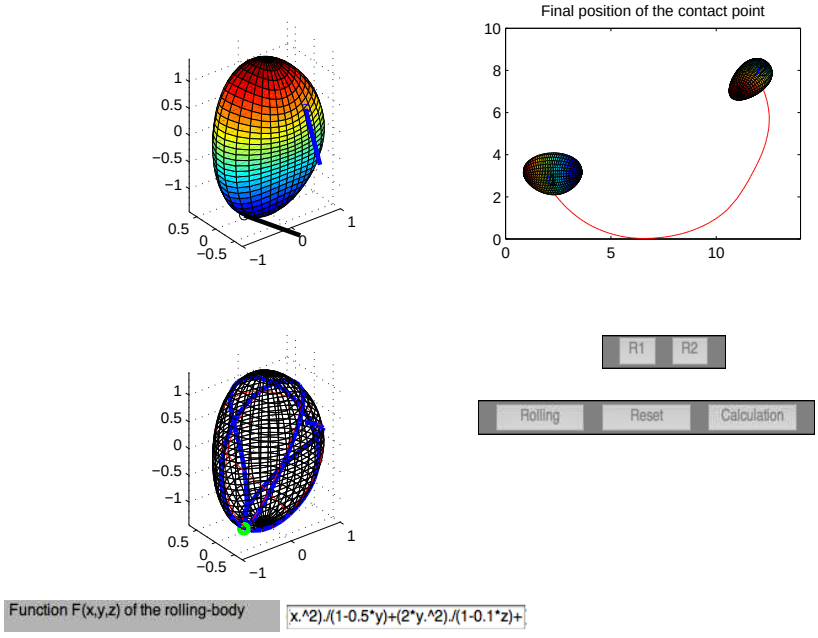

FIGURE 4.12 – Computation for adjusting the final position of contact point by continuation method ($s = 35$).

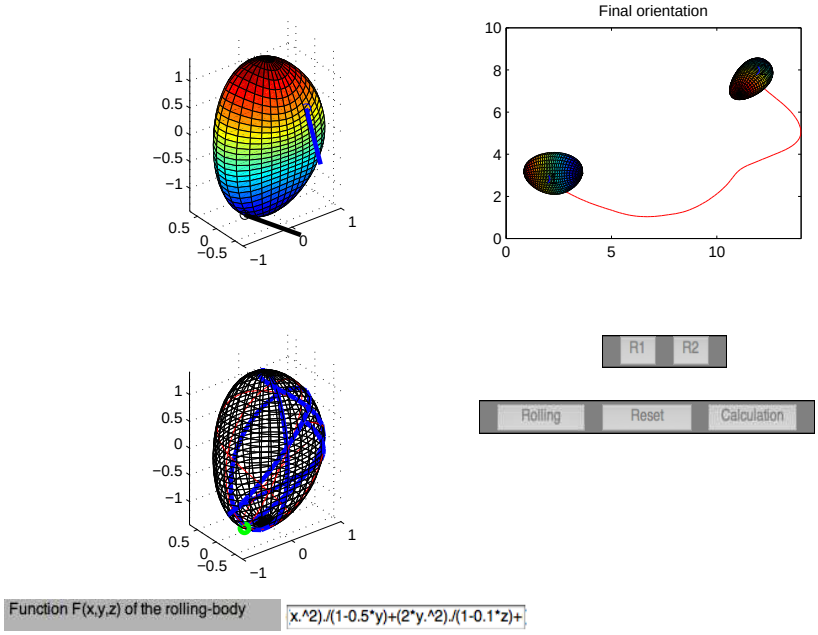

FIGURE 4.13 – Computation for adjusting the final orientation of the convex body by continuation method ($s = 70$).

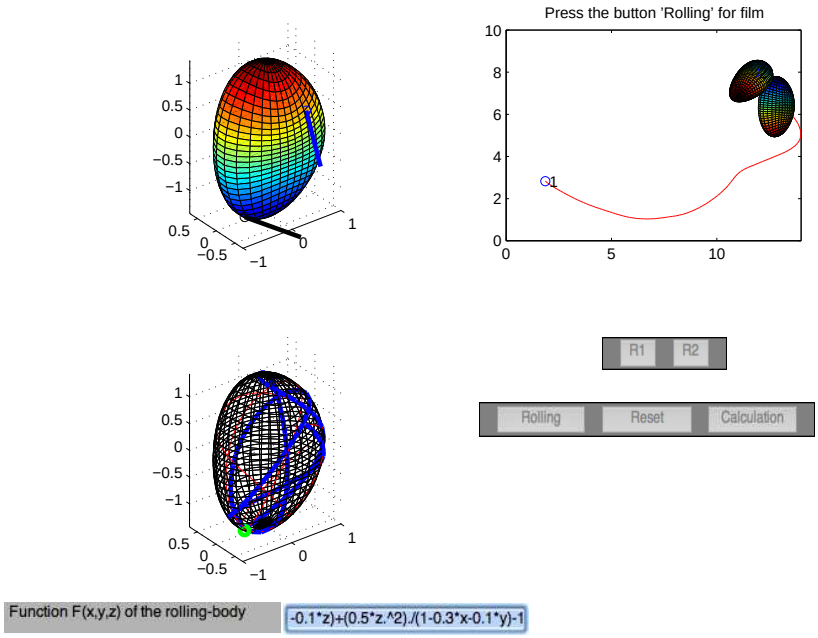

FIGURE 4.14 – Convex body rolling along the curve before reaching the final position.

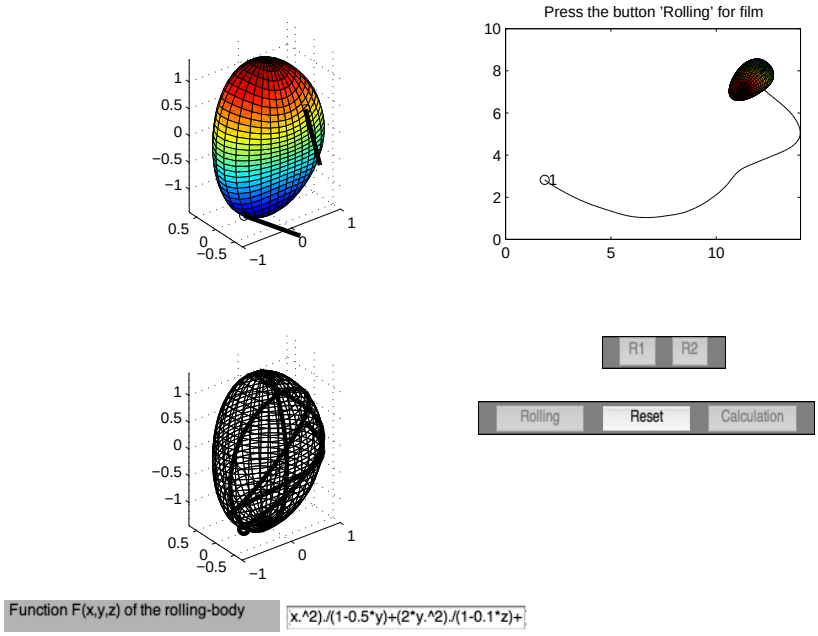

FIGURE 4.15 – Matching at the end of rolling.

4.6 Discussion and Conclusion

The main difficulty in the motion planning for convex bodies with rolling constraints relies on the fact that the displacement and the change of orientation cannot be dissociated one from the other. In the case of Problem **L1.**, every closed curve on S_1 can be associated with an element of the group $SE(2)$, and the concatenation of two closed curves corresponds to the group operation for $SE(2)$. This correspondence was implicitly mentioned in [66] via the Gauss-Bonnet Theorem, and it was explicitly and systematically explored in [15] for the construction of the lattice structure and basic actions. However, using this point of view, exact computations as presented in [66] cannot be extended beyond the plate-ball system, and approximate computations based on some discretization of the state space presented in [15] produce highly oscillating trajectories as they are obtained by concatenating a large number of basic actions composed of rolling along some closed curves defined on S_1.

In this paper, we have adopted a more global point of view which is to modify continuously, via the continuation method developed in [23, 25], an arbitrary non singular control (any plane curve which is not straight line in the case of problem **L1**) in order to achieve one control which steers the system from a given initial state to preassigned final state. We have implemented this method to solve the problem **L1-1** (rolling of general strictly convex bodies on the free plane). We have shown through several examples the robustness and the convergence speed of this method. It is worth pointing out that the only knowledge about the surface S_1 required by the numerical implementation of our method is the Gaussian curvature function K_1 of S_1. We have assumed in Section 4.4 that there exists a smooth function $f : \mathbb{R}^3 \to \mathbb{R}$ such that $S_1 = f^{-1}(0)$, then K_1 can be directly expressed (and numerically evaluated) from f. The numerical advantage of this *level-set* approach relies on the fact that our motion planning algorithm can be implemented without dealing with any change of local parameterization (chart) of S_1. We also note that this assumption is not restrictive. Indeed, for any compact

convex body S_1, if we assume that the origin 0 is inside of S_1, then we can define f as follows :

$$f(x) = t - 1, \quad \text{if } \frac{x}{t} \in S_1, \ t > 0. \tag{4.33}$$

Then, $S_1 = f^{-1}(0)$. Moreover, one can show that f is convex. Therefore, the Gaussian curvature can be computed from this function f since any continuous convex function admits second derivatives almost everywhere (cf. [47, Chap. I, Sect. 5]).

Our method can be adapted in order to solve **L1-2** (a convex body S_1 rolling on a plane with obstacles on the latter) by potential fields and this is the purpose of a forthcoming paper. Solving **L1-3** (strictly convex body S_1 rolling on a plane with prohibited regions on S_1) is more challenging since we must deal numerically with local charts of S_1. A possible way to address this issue is to use penalization techniques. An additional difficulty regarding **L2** (one strictly convex body rolling on the top of the other without or with prohibited regions) relies on the fact that the invertibility of $D\phi_p$ involved in the Path Lifting Equation (4.12) as well as the non-explosion condition require $K_2 - K_1 \neq 0$ at the contact point, but this condition may not be globally verified for two general smooth convex bodies.

4.7 Appendix : Continuation method applied to the rolling-body problem

For the sake of completeness, we summarize in this Appendix principal results regarding the **Condition 4.1** in the case of a strictly convex surface S_1 rolling on a plane. The reader can refer to [23] and references therein for a complete discussion on this issue. Roughly speaking, it is shown in [23] that if S_1 verifies a simple geometric property (see **Condition 4.2** below), then there exists a compact subset $\mathcal{K}$ in the state space M verifying the **Condition 4.1**, which is large enough to completely resolve the MPP.

The existence of a large compact $\mathcal{K}$ verifying the **Condition 4.1** requires a "small" singular set $\phi_p(S_p)$ characterized by Proposition 4.2. This condition is guaranteed by the existence of a periodic geodesic on S_1, stable for the geodesic flow of S_1. More precisely, let d_1 be the distance function associated to the Riemannian metric of S_1 induced by the usual metric of $\mathbb{R}^3$.

Condition 4.2. *We say that a surface S_1 verifies* **Condition 4.2** *if there exists a geodesic curve $\gamma : \mathbb{R}^+ \to T_1S_1$, $L > 0$ and $\rho_0 > 0$ such that*

(s) $\gamma(t + L) = \gamma(t)$ for all $t \geq 0$ (cf. [58]) *;*

(p) $\forall \rho < \rho_0$, $\exists \eta(\rho) > 0$, $\forall y_0 \in N_\rho(G)$, $\forall t \geq 0$, we have

$$\phi(y_0, t) \in N_\eta(G),$$

and

$$lim_{\rho \to 0} \eta(\rho) = 0,$$

where $G := \gamma([0, L])$, $N_\rho(G)$ is the open set of points $y \in T_1S_1$ such $d_1(y, G) < \rho$ and $\phi(y, t)$ is the geodesic flow of T_1S_1.

It is shown in [58] that **Condition 4.2** holds true for any convex compact surface having a symmetry of revolution and it is generic within the convex compact surfaces verifying $K_{\min}/K_{\max} > \frac{1}{4}$, where $K_{\min}$ and $K_{\max}$ denote the minimum and the maximum respectively of the Gaussian curvature over the surface.

Assume now that S_1 verifies **Condition 4.2** and let G be the support of the periodic geodesic. Then, $\rho \in (0, \rho_0)$, define $\mathcal{K}_{\bar{\rho}}$ as the set complement in T_1S_1 of $N_\rho(G) \times L$, where L is a fixed line in $\mathbb{R}^2$. The next proposition, proved in [23], tackles the non-explosion issue relative to the global existence of the solution of the Path Lifting Equation.

Proposition 4.4. *There exists a line $L \in \mathbb{R}^2$ and $\bar{\rho} > 0$ such that the corresponding $\mathcal{K}_{\bar{\rho}}$ verifies* **Condition 4.1**.

Then, we have the following proposition guaranteeing that the continuation method can be successfully applied for solving the rolling-body motion planning problem.

Proposition 4.5. *With above notations, for every path $\pi : [0, 1] \to \mathcal{K}_{\bar{\rho}}$ of class C^1 and every control $\bar{u} \in H$ such that $\pi(0) = \phi_p(\bar{u})$, the solution of the Path Lifting Equation (4.12), with initial condition equal to $\bar{u}$, exists globally over $[0, 1]$.*

We now describe how Proposition 4.5 can be applied to the rolling-body motion planning problem. Assume that one wants to roll the body from an initial position $p \in M$ to a final one $q \in M$.

Let us first assume that both p and q belong to $\mathcal{K}_{\bar{\rho}}$. We note that, since γ is periodic, $N_\rho(G)$ is diffeomorphic to the product of a small two-dimensional ball and a closed path on S_1. Therefore, $\mathcal{K}_{\bar{\rho}}$ is closed and arc-connected. We begin by taking an arbitrary control $\bar{u}$ which does not belong to S_p. Then we choose a C^1-path $\pi : [0, 1] \to \mathcal{K}_{\bar{\rho}}$ such that $\pi(0) := \phi_p(\bar{u})$ and $\pi(1) := q$. Proposition 4.5 guarantees that, by integrating Eq. (4.12) over $[0, 1]$ with initial condition equal to $\bar{u}$, we obtain a curve $\Pi : [0, 1] \to H$ such that $\phi_p(\Pi(s)) = \pi(s)$ for $s \in [0, 1]$. In particular, we have $\phi_p(\Pi(1)) = \pi(1) = q$, which means that the control $u := \Pi(1)$ solves the motion planning problem. If, for instance, p does not belong to $\mathcal{K}_{\bar{\rho}}$, it suffices first to roll the body along one geodesic which brings it to a point $\tilde{p}$ belonging to $\mathcal{K}_{\bar{\rho}}$, then we consider $\tilde{p}$ as the new initial condition, and the continuation method will apply. We recall that geodesic curves are admissible trajectories for the rolling body problem by Proposition 4.1.